

Optical Markers in Duodenal Mucosa Predict the Presence of Pancreatic Cancer

Yang Liu,¹ Randall E. Brand,² Vladimir Turzhitsky,¹ Young L. Kim,¹ Hemant K. Roy,² Nahla Hasabou,² Charles Sturgis,² Dhiren Shah,² Curtis Hall,² and Vadim Backman¹

Abstract Purpose: Pancreatic cancer remains one of the most deadly cancers and carries a dismal 5-year survival rate of <5%. Therefore, there is urgent need to develop a highly accurate and minimally invasive (e.g., without instrumentation of the pancreatic duct given high rate of complications) method of detection. Our group has developed a collection of novel light-scattering technologies that provide unprecedented quantitative assessment of the nanoscale architecture of the epithelium. We propose a novel approach to predict pancreatic cancer through the assessment of the adjacent periampullary duodenal mucosa without any interrogation of the pancreatic duct or imaging of the pancreas.

Experimental Design: Endoscopically and histologically normal-appearing periampullary duodenal biopsies obtained from 19 pancreatic cancer patients were compared with those obtained at endoscopy from 32 controls. Biopsies were analyzed using our newly developed optical technologies, four-dimensional elastic light-scattering fingerprinting (4D-ELF) and low-coherence enhanced backscattering (LEBS) spectroscopy.

Results: 4D-ELF- and LEBS-derived optical markers from normal-appearing periampullary duodenal mucosa can discriminate between pancreatic cancer patients and normal controls with 95% sensitivity and 91% specificity. Moreover, the diagnostic performance of these optical markers was not compromised by confounding factors such as tumor location and stage.

Conclusions: Here, we showed, for the first time, that optical analysis of histologically normal duodenal mucosa can predict the presence of pancreatic cancer without direct visualization of the pancreas.

Pancreatic cancer is the fourth most common cause of cancer death in the United States. It has one of the worst prognoses with an overall 5-year survival rate <5% and most patients dying within the first 2 years (1). The major reason for this dismal prognosis is due in a large part to the advanced stage of the disease at diagnosis. One approach to improving this grim prognosis is detecting the pancreatic adenocarcinoma early, when the tumor has not spread locally or metastasized and attempts at a curative resection are possible. However, at the present time, no effective screening technique for pancreatic cancer is available.

Other diseases have safely used routine endoscopy with mucosal biopsies for screening. For example, it is standard

practice to perform colonoscopy with biopsies in patients with ulcerative colitis for colon cancer surveillance (2) and upper endoscopy with biopsies in patients with Barrett's esophagus for esophageal cancer surveillance (3). Assessment of the duodenal mucosa adjacent to the ampulla to predict pancreatic cancer, and, thus, enable for the first time screening for pancreatic cancer in asymptomatic patients, represents an attractive approach due to its accessibility and straightforwardness. This approach poses the possibility of pancreatic cancer screening for patients with insidious nonspecific symptoms and overcomes one important hurdle of pancreatic cancer screening by avoiding any interrogation of pancreatic duct that could lead to significant complications. This approach is based on the potential "field effect" of pancreatic carcinogenesis. The field effect is the proposition that given the similar genetic and environmental milieu, a neoplastic lesion in a particular tissue site should also be detectable outside this location. Field effect has been a subject of intensive investigations in a number of gastrointestinal organs, notably the colon (4, 5), and has been used for the diagnosis of the presence of neoplastic lesions by means of optical spectroscopic measurements taken outside the spatial extent of the lesion (6, 7). A recent study reported the profound epigenetic alterations in the uninvolved normal-appearing duodenal mucosa from patients with a resected pancreatic cancer when compared with chronic pancreatitis patients (8), thus supporting the biological plausibility of duodenal mucosal interrogation as a screening/diagnostic test

Authors' Affiliations: ¹Biomedical Engineering Department, Northwestern University and ²Department of Internal Medicine, Evanston Northwestern Healthcare, Evanston, Illinois

Received 7/5/06; revised 10/4/06; accepted 11/30/06.

Grant support: National Science Foundation grant BES-0547480 and NIH grants R01CA112315.

The costs of publication of this article were defrayed in part by the payment of page charges. This article must therefore be hereby marked *advertisement* in accordance with 18 U.S.C. Section 1734 solely to indicate this fact.

Requests for reprints: Randall Brand, Department of Internal Medicine, Evanston Northwestern Healthcare, 2100 Pfingsten Road, Glenview, IL 650026. Phone: 847-657-1900; Fax: 847-657-1961; E-mail: rbrand@enh.org.

©2007 American Association for Cancer Research.

doi:10.1158/1078-0432.CCR-06-1648

for pancreatic cancer. This approach is attractive given the excellent patient acceptability and minimal complications of endoscopic duodenal evaluation (as opposed to the large number of complications inherent in instrumenting the pancreatic duct).

We have recently developed two complementary optical techniques, four-dimensional elastic light-scattering spectroscopy (4D-ELF) and low-coherence enhanced backscattering (LEBS) spectroscopy, that allow heretofore unattainable quantitative assessment of the nanoarchitecture/microarchitecture *in situ* (6, 7, 9–11). These techniques use the elastic light-scattering signals from tissue that exhibit characteristic structure-dependent signatures in wavelength (i.e., spectrum) and scattering angle. Both 4D-ELF and LEBS enable probing the depth-sensitive tissue organization at scales from tens of nanometers to microns; that is, from macromolecules to whole cells, and provide improved diagnosis when combined. Use of this technology has shown that 4D-ELF and LEBS have unprecedented sensitivity for the assessment of the genetic/epigenetic changes of the field effect of colon carcinogenesis, whereby 4D-ELF and LEBS examination of the uninvolved (i.e., endoscopically and histologically normal) mucosa of the rectal mucosa accurately predicted the presence of colonic neoplasia and allowed for the detection of colon carcinogenesis throughout the colon far earlier and more accurately than currently available molecular, genetic, or histologic markers (6, 7, 9, 10). In a similar spirit, the purpose of this current pilot study was to determine the feasibility of predicting pancreatic cancer through the assessment of normal-appearing periampullary duodenal mucosa without the need for direct imaging of the pancreas.

Materials and Methods

Human studies. The human studies were approved and done in accordance with the institutional review board at Evanston Northwestern Healthcare. After informed consent, 2- to 3-mm periampullary duodenal biopsies (within 1-3 cm of the ampulla) from normal-appearing mucosa were obtained from 19 pancreatic cancer patients, either immediately (within 30 min) after surgery from the resected portions of the duodenum or at the time of an endoscopic procedure, and compared with similar-sized periampullary duodenal biopsies obtained from 32 normal controls at the time of a routine endoscopic procedure. The control group consisted of those patients without any personal history of cancer or pancreatic disease or a significant family history of cancer. The pancreatic cancer group was defined as patients with histologically confirmed pancreatic adenocarcinoma. In addition, biopsies were also obtained from the distal duodenal mucosa (~10 cm from the ampulla) and the stomach of nine control and four pancreatic cancer patients out of the above 51 patients to examine the spatial extent of the field effect. All biopsies were placed in PBS. 4D-ELF and LEBS analyses were done within 2 h of tissue acquisition by observers blinded to clinical/endoscopic data. The biopsies were oriented so that the superficial mucosa was examined. The absence of histologic abnormalities in tissue biopsied from the periampullary mucosa was also confirmed after the completion of 4D-ELF and LEBS measurements by a pathologist.

4D-ELF/LEBS instrument. The 4D-ELF and LEBS signals are simultaneously obtained using the same instrument. We have previously reported the development of 4D-ELF/LEBS instrument to obtain the comprehensive depth-sensitive light-scattering signatures from living tissue (7, 11). Briefly, the linearly polarized and collimated white light (divergence angle ~0.03°) from Xe lamp (Oriel) illuminates the tissue surface (~1.5 mm across). Tissue microstructures/nanostructures scatter the light in a wide range of backscattering

angles at various wavelengths. The scattered light was collected by a spectrograph (Acton Research) coupled with a charge coupled device camera (VersArray^{XP}, Roper Scientific). The camera records a two-dimensional image with the horizontal axis corresponding to the scattering wavelength λ (400-700 nm) and vertical axis corresponding to the scattering angle θ (-7° to 7°) for any given azimuthal angle ϕ . Furthermore, the instrument allows the measurement of two independent polarization components of the scattered light intensity with polarization parallel (I_{\parallel}) and orthogonal (I_{\perp}) to that of the incident light. In each 4D-ELF/LEBS measurement, the backscattering data were collected from ~2-mm² area of human biopsy. For each biopsy, light-scattering data were recorded from approximately seven different tissue sites that span the entire surface.

4D-ELF. 4D-ELF allows acquisition of light-scattering data in several dimensions. The four dimensions include the following: (a) wavelength of light λ , (b) the scattering angle θ (i.e., the angle between the backward direction and the direction of the propagation of scattered light), (c) azimuthal angle of scattering ϕ (i.e., the angle between the incident light polarization and the projection of the direction of the scattered light propagation onto the plane), and (d) polarization of scattered light p . 4D-ELF signals primarily originate from single-scattering and low-order scattering and contain information about the tissue structures with sizes ranging from submicron to several microns. Furthermore, the 4D-ELF differential polarization signal ($\Delta I = I_{\parallel} - I_{\perp}$) is particularly sensitive to the superficial tissue (e.g., epithelium and mucosa; refs. 11–14). The depth selectivity of polarization gating was previously confirmed in our experiments with physical tissue model, bioengineered tissue models, and Monte Carlo simulations (11–13).

Low-coherence enhanced backscattering. The angular distribution of the 4D-ELF features an enhanced backscattering (EBS) peak at the center of angular profile (approximately between -0.5° and 0.5°), known as LEBS peak, generated by the self-interference of light propagation in a random medium, such as biological tissue (15). Although conventional EBS in nonbiological medium has been extensively studied, it has been extremely difficult to investigate EBS in biological tissue due to the extremely narrow EBS peak in biological tissue. LEBS overcomes the limitation of conventional EBS for tissue characterization by combining the EBS measurements with low spatially coherent, broadband illumination, and spectrally resolved detection (15, 16). LEBS offers several advantages over conventional EBS, including significant broadening of an EBS peak, speckle reduction, depth selectivity, and wavelength-dependent spectroscopic information. The LEBS peak can be assessed in both angular and spectral dimensions. A single LEBS peak contains light-scattering signals originating from a wide range of tissue depth and allows the acquisition of the depth-sensitive information (16). Thus, the analysis of the spectral profile of the LEBS peak provides quantitative information about the structure of epithelial tissue at each tissue depth from 20 to 300 μ m (16). Furthermore, LEBS signals primarily depend on the second-order scattering of weakly localized photons by tissue structures. This contrast mechanism is unique to LEBS and cannot be probed by any other existing techniques.

Optical markers. To quantitatively characterize the epithelial tissue architecture at scales from tens of nanometers to several microns, we assessed a series of quantitative optical markers previously validated for diagnosis of colon carcinogenesis: 4D-ELF spectral slope, fractal dimension of tissue microarchitecture (obtained by 4D-ELF), full width at half maximum (FWHM) of LEBS angular peak, LEBS enhancement factor, and LEBS autocorrelation decay rate. These markers were selected because they were previously shown to be highly diagnostic for detecting colon carcinogenesis far earlier than any other existing techniques (6, 7, 9, 10).

A light-scattering spectrum $\Delta I(\lambda)$ obtained by 4D-ELF is generally a declining function of wavelength and its steepness is related to the size distribution of the scattering structures of different sizes ranging from 40 to 800 nm. The steepness is quantified as the coefficient of the linear fit to $\Delta I(\lambda)$, referred to as the "spectral slope." The spectral slope serves

as a quantitative and easily measurable marker of the structural distribution within the cells.

The angular distributions of the 4D-ELF signatures were used to calculate the fractal dimension of tissue microarchitecture, which characterizes cell structures at scales $>1 \mu\text{m}$. To estimate the fractal dimension, the angular distribution $\Delta I(\theta)$ at 550 nm was first Fourier transformed to generate the two-point mass density correlation $C(r) = [\rho(r)\rho(r+r')]$, where $\rho(r)$ is the local mass density at the spatial point r , which is proportional to the concentration of intracellular solids, such as DNA, RNA, and proteins. At all tissue sites, $C(r)$ was approximated as the power-law (ref. 17; $C(r) = r^{D-3}$) for r ranging from 1 to 50 μm , where D is referred to as fractal dimension. D was obtained from the linear slope of $C(r)$ in the log-log scale.

The EBS peak at the center of angular distribution (i.e., LEBS peak) can be assessed in both angular and spectral dimensions. The angular profile of LEBS peak $I_{\text{LEBS}}(\theta)$ was used to calculate two other optical markers, the LEBS FWHM and LEBS enhancement factor, which are sensitive to optical properties of tissue architecture, such as scattering coefficient and absorbance. The peak width of LEBS is characterized as the FWHM of the LEBS peak $I_{\text{LEBS}}(\theta)$ averaged within wavelength range from 620 to 670 nm. LEBS enhancement factor is defined as the ratio of the LEBS peak intensity $I_{\text{LEBS}}(\theta = 0^\circ)$ to the incoherent baseline intensity $I_{\text{BASE}}(\theta)$ outside of the LEBS peak, which was measured for large angles of backscattering ($\theta > 3^\circ$) at the same wavelength range.

The spectral behavior of the LEBS signal primarily depends on the second-order scattering of weakly localized photons by tissue structures, which is a unique contrast mechanism that cannot be probed by other existing techniques. The spectrally resolved LEBS signals were normalized as follows: $I_{\text{EBS}}(\theta, \lambda) = (I(\theta, \lambda) - I_{\text{BASE}}(\lambda)) / I_{\text{REF}}(\lambda)$, where I_{BASE} is the baseline (incoherent) intensity and I_{REF} is the reference intensity collected from a reflectance standard (Ocean Optics; this normalization accounted for the nonuniform spectrum of the incident light illumination and the spectral response of detection). Generally, the spectral profile $I_{\text{EBS}}(\lambda)$ of LEBS peak is a declining oscillatory function of wavelength, consisting of high-frequency oscillatory features $I_{\text{EBS}}^{\text{HIGH}}(\lambda)$ on top of the low-frequency declining profile $I_{\text{EBS}}^{\text{LOW}}(\lambda)$. The high-frequency component was extracted by subtracting the low-frequency profile from LEBS spectrum [$I_{\text{EBS}}^{\text{HIGH}}(\lambda) = I_{\text{EBS}}(\lambda) - I_{\text{EBS}}^{\text{LOW}}(\lambda)$]. More specifically, the original spectrum $I_{\text{EBS}}(\lambda)$ first subtracted the corresponding fourth-order polynomial [i.e., $I_{\text{EBS}}^{\text{LOW}}(\lambda)$] to extract the high-frequency fluctuating component. The resulting spectrum $I_{\text{EBS}}^{\text{HIGH}}(\lambda)$ arises from the interference of photons reflected from refractive index fluctuations within a scattering medium and is linked to the tissue nanostructural/microstructural refractive index variation. Its autocorrelation function was calculated from $C(\Delta k) = [I_{\text{EBS}}^{\text{HIGH}}(k)I_{\text{EBS}}^{\text{HIGH}}(k + \Delta k)] / [I_{\text{EBS}}^{\text{HIGH}}(k)I_{\text{EBS}}^{\text{HIGH}}(k)]$, where k is the wave number ($k = 2\pi/\lambda$). The logarithm of the correlation function $\ln[C(\Delta k)]$ is linearly dependent on $(\Delta k)^2$ (refs. 18, 19). The corresponding slope of its linear fit is referred to as the LEBS autocorrelation decay rate.

For all LEBS markers, the depth of penetration of LEBS signals was chosen to be $\sim 70 \mu\text{m}$ [spatial coherence length $L_{\text{sc}} = 110 \mu\text{m}$ and $I_{\text{EBS}}(\theta = 0^\circ)$; ref. 6]. This penetration depth ensures probing of the entire epithelial layer with minimal signal contamination from underlying diagnostically less significant tissue components. The penetration depth was also found to provide the most diagnostic information in our previously published results on the diagnosis of colon carcinogenesis (6).

Statistical analysis. Statistical analysis was done using Microsoft Excel and SAS statistical software package (SAS Institute, Inc.). Each optical marker was compared between control and pancreatic cancer patients using the Student's t test. The effects of age on each optical marker were analyzed with two-way ANOVA and correlation. Two-sided P values were used for all analyses. A two-sided P value <0.05 was considered as statistically significant. The performance characteristics (i.e., sensitivity and specificity) with all optical markers combined were calculated using logistic regression. The diagnostic accuracy was further evaluated by the leave-one-out cross-validation.

Results

Patient demographics. The age was 50 ± 15 years (mean \pm SD) for the 32 control patients and 70 ± 12.1 years for the 19 pancreatic adenocarcinoma patients. Staging for the pancreatic cancer patients was as follows: stage I, two patients; stage II: eight patients; stage III: two patients; and stage IV: seven patients. Approximately 75% of patients were female in each group. Eight of the pancreatic cancer patients underwent surgical resection.

Light-scattering fingerprinting. Light-scattering 4D-ELF/LEBS signatures exhibit characteristic structure and optical property-dependent patterns, referred to as "fingerprints," and provide the most comprehensive depth-sensitive quantitative information about light-scattering properties of tissue. Figure 1 shows the representative light-scattering fingerprints from periamпуляр duodenal mucosa recorded from normal control and pancreatic cancer patient. The fingerprints reveal a dramatic qualitative difference in the scattering patterns, reflecting the tissue architectural alterations at scales from tens of nanometers to several microns. To quantitatively characterize the changes in light-scattering signatures and tissue structures, we analyzed a series of optical markers.

Changes in 4D-ELF-derived optical markers. A number of optical markers, in particular, the 4D-ELF spectral slope and fractal dimension, were extracted to characterize the specific properties of cell structure. As discussed in Materials and Methods, the wavelength-dependent light-scattering spectra $\Delta I(\lambda)$ were used to calculate the spectral slope, which evaluates the size distribution from macromolecules to organelles. Typically, the abundance of small scatterers (up to 60 nm) increases the spectral slope (7). Figure 2A shows the alteration of the spectral slope obtained from uninvolved (histologically and endoscopically normal) periamпуляр duodenal mucosa in all pancreatic cancer patients and pancreatic cancer patients with resectable tumors compared with those who were normal controls. The spectral slope is significantly lower for patients with pancreatic cancer ($P = 0.02$), indicating that the relative portion of larger structures increases in tissue nanoscale/microscale organization for cancer patients. Furthermore, as shown in Fig. 2A, the decrease in the spectral slope from

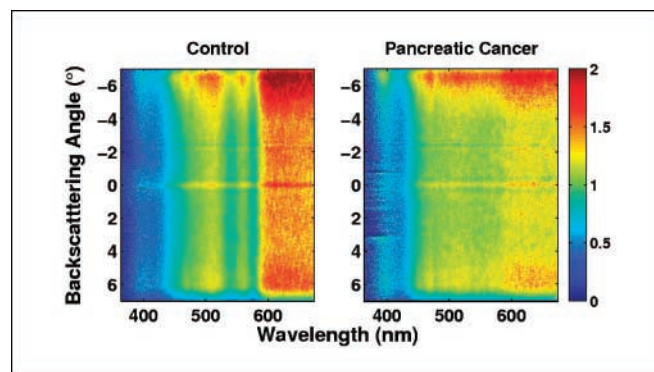


Fig. 1. Representative light-scattering fingerprints from periamпуляр duodenal mucosa of control subjects and patients with pancreatic adenocarcinoma. The color represents the backscattering intensity. Horizontal axis, the wavelength of backscattering light; vertical axis, the backscattering angle. The fingerprints show a significant difference between controls and patients with pancreatic adenocarcinoma.

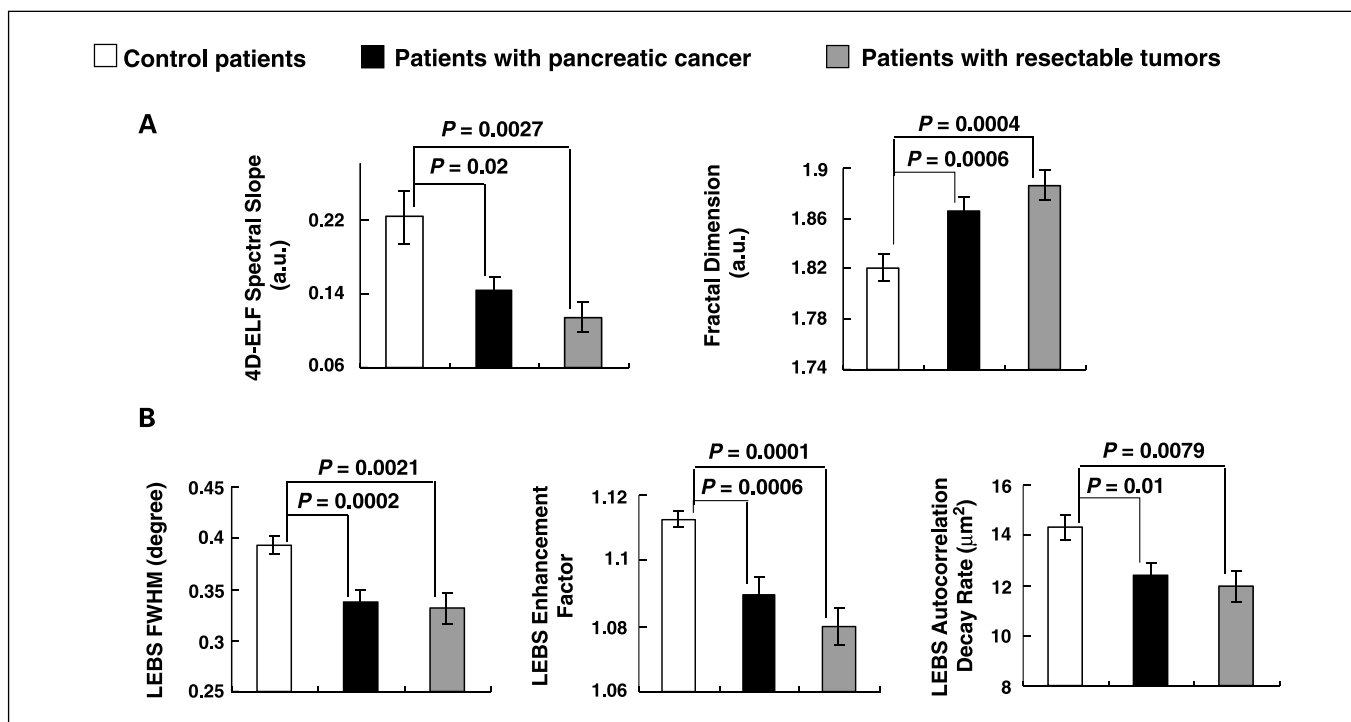


Fig. 2. 4D-ELF- and LEBS-derived optical markers obtained from endoscopically and histologically normal duodenal periampullary mucosa enable diagnosis of pancreatic carcinogenesis without the need for interrogation or direct visualization of the pancreas. **A**, 4D-ELF-derived optical markers: spectral slope and fractal dimension from the periampullary duodenal mucosa. The 4D-ELF spectral slope in pancreatic cancer patients was significantly lower than that in the controls ($P = 0.02$). Such decrease was also significant in pancreatic cancer patients with resectable tumors ($n = 11$; $P = 0.0027$). The fractal dimension assessed from patients with pancreatic cancer and resectable tumors was significantly higher compared with that from the control group ($P \leq 0.0006$). **B**, LEBS-derived optical markers: LEBS FWHM, LEBS enhancement factor, and LEBS autocorrelation decay rate from the periampullary duodenal mucosa drastically decreased in patients with pancreatic cancer and resectable tumors ($P \leq 0.01$). Bars, SE. Resectable tumors include resectable and appearing-to-be-resectable tumors.

patients with resectable tumors was found to also be statistically significant ($P = 0.0027$).

Fractal dimension was assessed from the angular distribution of light-scattering signatures and is an independent variable to characterize the tissue organization at larger length scale, ranging from large organelles to groups of cells. As shown in Fig. 2A, the fractal dimension is significantly elevated in the periampullary duodenal mucosa of both pancreatic cancer patients ($P = 0.0006$) and those with resectable tumors ($P = 0.0004$). This suggests denser organization of cellular structures.

Changes in LEBS-derived optical markers. Three LEBS markers were assessed, including the LEBS peak width (FWHM), LEBS enhancement factor, and the autocorrelation decay rate of LEBS spectra, as discussed above in Materials and Methods. Figure 2B shows the LEBS markers assessed in endoscopically normal-appearing periampullary duodenal mucosa of normal controls and pancreatic cancer patients. There was a dramatic decrease in both the LEBS FWHM and enhancement factor in patients with pancreatic adenocarcinoma when compared with normal controls ($P = 0.0002$ for LEBS FWHM and $P = 0.0006$ for enhancement factor; Fig. 2B). This suggests a decreased scattering coefficient and absorbance in periampullary duodenal mucosa for pancreatic cancer patients. The significantly decreased autocorrelation decay rate in patients with pancreatic cancer implies more disordered nature of intracellular density fluctuations in periampullary duodenal mucosa in patients with pancreatic cancer ($P = 0.01$; Fig. 2B).

Furthermore, all LEBS markers are effective in differentiating the control patients from pancreatic cancer patients with resectable tumors ($P = 0.0021$, 0.0001 , and 0.0079 for LEBS FWHM, enhancement factor, and LEBS autocorrelation decay rate, respectively).

Performance characteristics. The performances obtained by combining all five optical markers (i.e., 4D-ELF spectral slope, fractal dimension, LEBS FWHM, LEBS enhancement factor, and LEBS autocorrelation decay rate) for discriminating normal control patients from pancreatic cancer patients and pancreatic cancer patients with resectable tumors were excellent, with 95% sensitivity, 91% specificity and 100% sensitivity, 94% specificity, respectively (Table 1). This performance characteristic was obtained by logistic regression with all five markers included. Leave-one-out cross-validation results in 84% sensitivity, 84% specificity for discriminating pancreatic cancer patients and normal controls and 100% sensitivity, 90% specificity for discriminating pancreatic cancer patients with resectable tumors and control patients.

4D-ELF/LEBS diagnosis is not compromised by confounding factors. Given that age and smoking history are important risk factors in developing pancreatic cancer, we wanted to ensure that the changes in 4D-ELF and LEBS-derived optical markers detect carcinogenesis itself rather than a mere age difference and smoking history among patients with pancreatic cancer and control subjects. To address this question, we investigated how the optical markers vary with patients' age and smoking history. The effect of patients' age was addressed by means of

the following two types of studies: correlation and ANOVA analyses. First, we calculated the correlation coefficient between each optical marker and age. As shown in Table 2, none of the five markers strongly correlates with age. Second, we dichotomized patients' age at <60 and ≥60 years. As conventionally done, we used the two-way ANOVA to measure the differences between controls versus pancreatic cancer patients as well as between age groups. The analysis shows that age is not significantly associated with most of the five optical markers ($P = 0.06, 0.72, 0.91, 0.83,$ and 0.03 for 4D-ELF spectral slope, fractal dimension, LEBS autocorrelation rate, LEBS FWHM, and LEBS enhancement factor, respectively). Similarly, we found that all of five optical markers have no correlation with smoking history ($P = 0.17, 0.14, 0.37, 0.94,$ and 0.20 for 4D-ELF spectral slope, fractal dimension, LEBS autocorrelation rate, LEBS FWHM, and LEBS enhancement factor, respectively). Therefore, the changes in the optical markers are unlikely to be attributed to difference in age and smoking history in the patient population.

4D-ELF/LEBS diagnosis is not compromised by tumor location. As shown in Fig. 3, several optical markers obtained from the periampullary duodenum are significant even for tumors located in the body and tail of the pancreas.

Spatial extent of field effect in pancreatic cancer. To determine the limit of the spatial extent of the field effect in pancreatic cancer, we obtained 4D-ELF/LEBS readings from two nonperiampullary sites: the gastric mucosa along the lesser curvature of the stomach and the distal duodenum ~ 10 cm from the ampulla of Vater. We found that none of five optical markers discussed above was statistically significant when measured from the stomach tissue (Fig. 4). Moreover, in the distal duodenum, the optical markers were also not significant, although some P values were lower than those from the stomach.

Histologic review of the specimens. Histologic review of the periampullary duodenal specimens found that the vast majority 47 of 51 were normal. Of the remaining four specimens, two healthy controls and one pancreatic cancer patient (stage IV) had mild chronic inflammation, and one healthy control had mild acute and chronic inflammation. For the other sites (distal duodenum and stomach), all biopsies were normal except for one healthy control having superficial chronic gastritis.

Table 1. The performance characteristics of diagnosis of all pancreatic cancer patients and patients with resectable tumors by means of 4D-ELF/LEBS examination of periampullary duodenal mucosa

	Sensitivity (%)	Specificity (%)
Control vs pancreatic cancer patients	95	91
Control vs pancreatic cancer patients with resectable tumors	100	94

NOTE: The performance characteristics of individual 4D-ELF/LEBS markers is compared with those obtained when all 4D-ELF/LEBS markers are combined. The high level of performance was only attainable when all five markers were included.

Table 2. Effect of age on the 4D-ELF/LEBS-derived optical markers recorded from the periampullary duodenal mucosa

Optical marker	Correlation coefficient, control	Correlation coefficient, cancer
4D-ELF spectral slope	0.43*	-0.025
Fractal dimension	-0.005	0.049
LEBS autocorrelation decay rate	-0.096	0.31*
LEBS FWHM	0.14	-0.48
LEBS enhancement factor	0.021	-0.39

NOTE: The correlation coefficients between age and optical markers were stratified by diseases (control versus pancreatic cancer). The correlation coefficient was calculated using linear regression with the individual optical marker as the dependent variable and age as the predictor.

*This optical marker decreases in pancreatic cancer patients' group. Therefore, the slight positive correlation (i.e., this optical marker increases with age) indicates that if the risk of developing pancreatic cancer increases with older age, this marker would be more efficient in differentiating control and pancreatic cancer in patients with older age.

Discussion

We show herein, for the first time, by the use of 4D-ELF- and LEBS-derived optical markers, the possible existence of a field effect for pancreatic cancer in endoscopically and histologically normal-appearing adjacent periampullary duodenal mucosa. The results of this pilot study show the feasibility of diagnosing pancreatic cancer by means of examination of periampullary duodenal mucosa without direct visualization of the pancreas. 4D-ELF and LEBS are remarkably sensitive to the changes in tissue nanoarchitecture/microarchitecture, which are otherwise undetectable with other imaging modalities, including histologic analysis. The quantitative optical markers obtained from the 4D-ELF and LEBS analysis in human periampullary duodenal biopsies were able to distinguish pancreatic cancer patients from normal controls with 95% sensitivity and 91% specificity. Furthermore, for technique to be clinically significant, it has to be able to differentiate tumors at potentially resectable stage, which was defined in our study as a stage I or II lesions. Interestingly, the sensitivity and specificity was even greater for this subset of patients (100% and 94%, respectively). The data indicate that both 4D-ELF and LEBS provide complementary diagnostic information. The compelling diagnostic performance suggests the potential of this technique for pancreatic cancer screening.

The diagnostic performance of this optical technology did not appear to be compromised by confounding factors such as age, tumor location, tumor size, or tumor stage. Histologic examination of the duodenal biopsies confirmed that no microscopic changes such as inflammation or presence of cancer cells were responsible for the optical findings because only mild inflammatory changes were seen in four patients, only one of whom had pancreatic cancer. Although our sample size was not large, the statistical analyses (i.e., correlation and two-way ANOVA) show that the changes in the optical markers are unlikely to be attributed to differences in age and smoking history in the study population. However, due to the fact that,

in our pilot study, the average age of the control group was 20 years lower than that of the pancreatic cancer group, it will be essential in future large-scale studies to have a better balanced age distribution to allow for accurate quantification of the effect of age on optical markers. These large-scale studies will also need to control for additional factors such as other pancreatic and biliary diseases (i.e., cholangitis, and acute and chronic pancreatitis), jaundice, weight loss, smoking history, and presence of biliary stents.

We also investigated the potential of the optical markers obtained from periampullary duodenal tissue to detect not only the most proximal pancreatic neoplasms (i.e., those located in the head and neck of the pancreas in the proximity to the ampulla), but also more distal lesions located in the body and tail of the pancreas. The results provide further support that 4D-ELF- and LEBS-derived optical markers are capable of accurately predicting pancreatic cancer, even for tumors located away from the ampulla. Because a reasonable goal for early detection is either a resectable tumor or a small tumor <2 cm in size, the data were analyzed to determine if size or stage (resectable versus unresectable) affected detection of the tumor. Although the numbers were small, several optical markers obtained from the periampullary duodenum are significant for resectable tumors and small tumors (≤ 2 cm; data not shown). The modest increase in *P* values for some of the optical markers for small or distally located tumors might be due to a small number of patients with tumors located in the body and tail ($n = 4$).

Our results suggest that there are a series of cellular nanostructural/microstructural and organizational changes in the periampullary duodenal mucosa of pancreatic cancer patients. The steeper 4D-ELF spectral slope seen in pancreatic cancer patients (Fig. 2A) shows that the size distribution of submicron intracellular structures shifts to larger sizes (7, 9). We have previously shown similar alterations in spectral slope in the initial stage of colon carcinogenesis in animal models and in human subjects with colorectal adenoma and adenocarcinoma (7, 9, 10). The increased fractal dimension in pancreatic cancer patients (Fig. 2A) reveals the denser distribution of cell organization at large scales, ranging from large organelles to groups of cells (7, 9). Other groups have reported similar increase in fractal dimension in rat esophageal cancer at a dysplastic stage (20). Furthermore, it has been reported by our group that the fractal dimension was elevated in colon carcinogenesis at a time point far earlier than the development of other conventional biomarkers (7, 10). The lower values seen in the LEBS FWHM and enhancement factor (Fig. 2B) indicate a lower scattering coefficient in the periampullary duodenal mucosa of pancreatic cancer patients. The decreased LEBS autocorrelation decay rate (Fig. 2B) in the pancreatic cancer patients reflects the stronger degree of disorder in nanostructural/microstructural refractive index fluctuation. The changes in disorder strength of duodenal mucosa in pancreatic cancer patients may be attributed to the increased concentration of intracellular macromolecular complex. We have previously identified similar increased disorder strength in

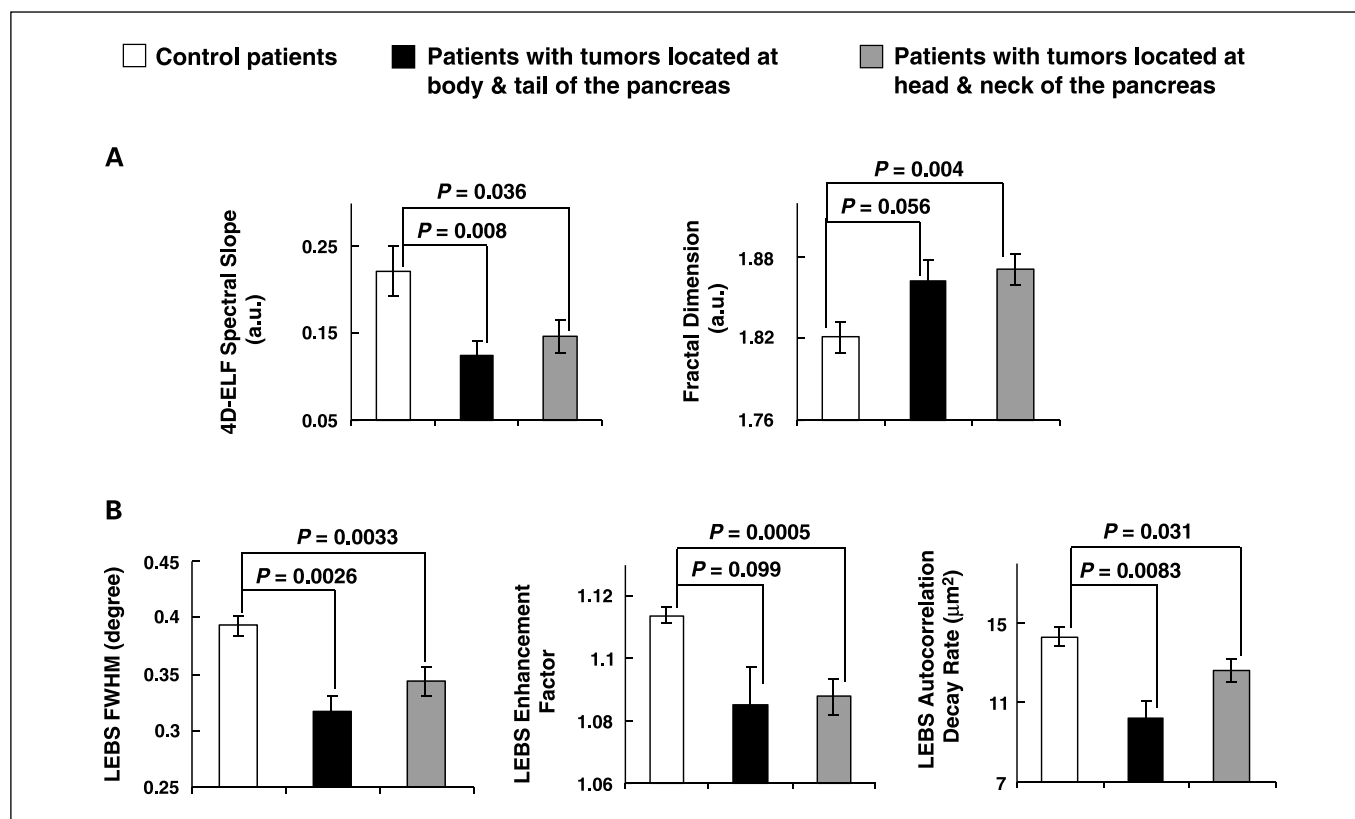


Fig. 3. The effect of tumor location on the 4D-ELF (A) and LEBS (B) optical markers obtained from the periampullary duodenum. These markers are significant not only for pancreatic tumors located most proximally to the ampulla (i.e., head and neck of the pancreas, $n = 15$) but also for the most distally (i.e., body and tail of the pancreas, $n = 4$) located tumors. Bars, SE.

colonocytes at the initial stage of colon carcinogenesis in azoxymethane-treated rat model (21). These changes in 4D-ELF- and LEBS-derived optical markers characterize the statistical alterations of cellular structures, which are the results of highly complex biological processes associated with numerous molecular, genetic, and morphologic events. As previously mentioned, these same optical markers have been identified to be highly diagnostic in predicting the field effect of colon carcinogenesis by means of assessment of colonoscopically normal rectal tissue (6). Interestingly, our data indicate that when assessed in periampullary mucosa, these markers are diagnostic for pancreatic neoplasia.

We also evaluated whether the changes in optical markers were confined to the periampullary duodenal mucosa in pancreatic cancer patients or were more diffuse in nature. Although caution in interpretation of these data is necessary due to the small sample size, the results suggest that the field effect is most pronounced adjacent to the ampulla when compared with the stomach and distal duodenum. This finding is consistent with our hypothesis that the duodenal mucosa is altered by tumor factors through either the pancreatic juice or shared vasculature.

The biological plausibility of the heretofore undescribed nanoarchitectural/microarchitectural changes associated with the field cancerization in the pancreas is supported by several lines of evidence. From a morphologic perspective, this is indicated by the almost uniform occurrence of PanIN lesion distant from a pancreatic cancer (22). Genetically, detection of *K-ras* mutations is commonly seen in patients at risk of pancreatic cancer but before the development of a frank cancer (23). Biochemically, markers such as glycoprotein moieties suggest that in patients with pancreatic cancer, there are diffuse

alterations throughout the pancreatic duct (24). Perhaps the strongest support for the field effect concept comes from a recent study by Matsubayashi et al. (8), which showed that pancreatic cancer patients have increased tendency to methylate genes in normal duodenum when compared with normal duodenum from chronic pancreatitis patients. In this study, DNA methylation patterns of 24 genes were determined in adenocarcinoma and chronic pancreatitis patients that had undergone pancreaticoduodenectomy. Even after adjusting for patient age, overall DNA methylation was more common on average for the 24 genes in the patients with pancreatic adenocarcinoma. Although we have previously shown that distinct genetic alterations have optically detected microarchitectural consequences (9), the present study does not address whether the epigenetic changes noted by Matsubayashi and his associates were responsible for change in optical markers. However, their study does underscore the biological plausibility of our findings by confirming alterations in the duodenal mucosa using standard molecular biological techniques. The reasons for changes in duodenal mucosa need to be explored in future studies.

Limitations of this initial study include the modest number of patients in this study. As mentioned previously, despite no statistical evidence of an age effect on these markers, the large difference in age between controls and pancreatic cancer patients leaves open the possibility (albeit unlikely) of residual confounding. In future studies, we will also evaluate benign pancreatic and biliary diseases to further define the specificity of these markers. Furthermore, we will use a large training and testing set to mitigate any concerns, albeit unlikely, about overfitting of data. The current study is unable to compare optical approaches to radiology because cancer patients were

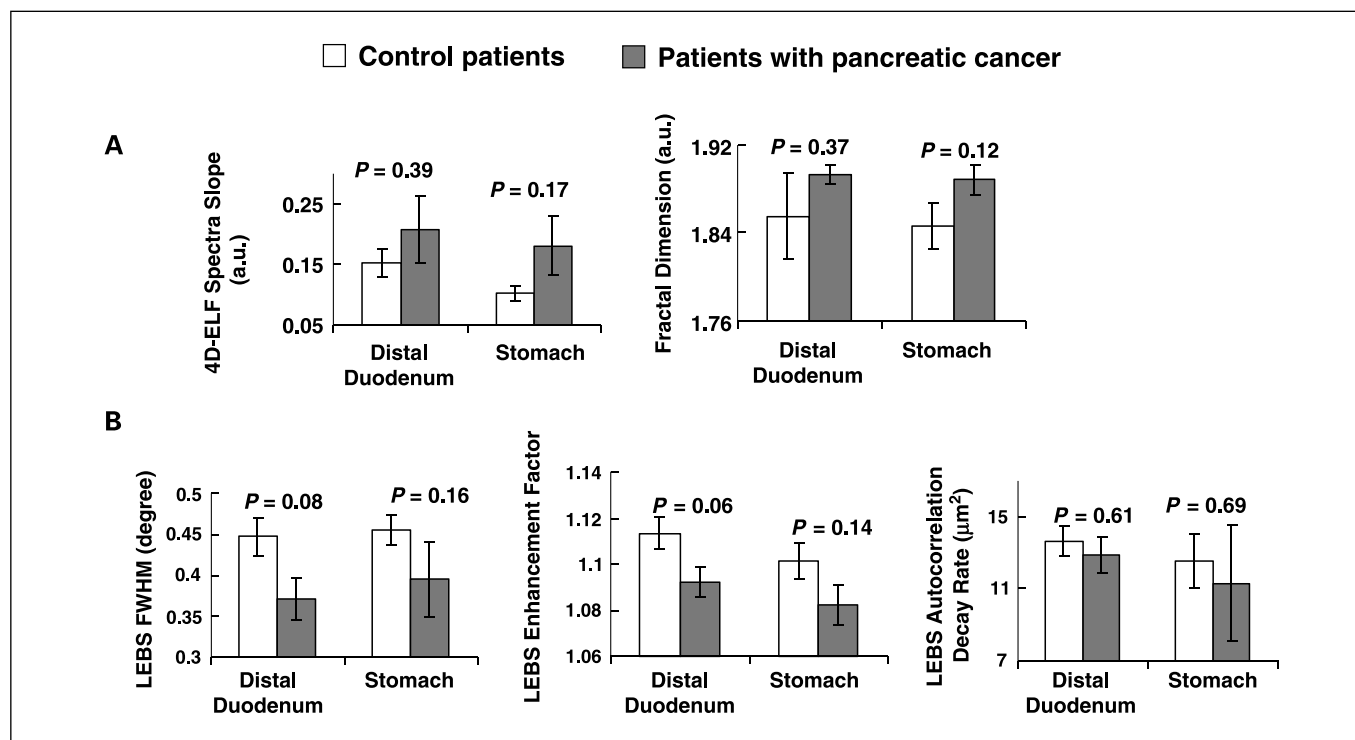


Fig. 4. Spatial extent of 4D-ELF (A) and LEBS (B) markers obtained from distal duodenal (~ 10 cm from the ampulla of Vater) and gastric mucosa. All optical markers are not significant for pancreatic cancer, indicating that the field effect associated with the pancreatic cancer does not spread to the distal duodenum and stomach. Bars, SE.

identified through abnormal imaging studies. Given that duodenal spectral evaluation identified small (resectable) pancreatic tumors, it is conceivable that this approach may allow diagnosis of tumors before them becoming radiologically evident. This study will not only attempt to validate these optical markers, but also evaluate for additional markers if the performance characteristics need to be improved by using the vast amount of unused information contained in light-scattering signatures.

In conclusion, we report, for the first time, that optical markers obtained by our techniques, 4D-ELF and LEBS, are able to accurately predict pancreatic cancer through the assessment of normal periampullary duodenal mucosa without the need

for any interrogation of the pancreatic duct or imaging of the pancreas. The diagnostic performance seen in this pilot study was not compromised by age, smoking history, tumor location, tumor stage, and tumor size. This approach can potentially revolutionize screening for pancreatic cancer by providing a highly accurate, minimally invasive means of risk assessment, thus determining which patients need intensive radiological assessment. This approach becomes even more clinically attractive given the advent of ultrathin endoscopes allowing upper endoscopy to be done safely without discomfort or need for sedation. Future large-scale clinical studies will be done to validate this potentially paradigm-shifting data on pancreatic cancer screening.

References

- Jemal A, Murray T, Ward E, et al. Cancer statistics 2005. *CA Cancer J Clin* 2005;55:10–30.
- Itzkowitz SH, Harpaz N. Diagnosis and management of dysplasia in patients with inflammatory bowel diseases. *Gastroenterology* 2004;126:1634–48.
- Boyce GA. Endoscopic evaluation of the patient with esophageal carcinoma. *Chest Surg Clin N Am* 1994;4:257–68.
- Braakhuis BJM, Tabor MP, Kummer JA, Leemans CR, Brakenhoff RH. A genetic explanation of Slaughter's concept of field cancerization: evidence and clinical implications. *Cancer Res* 2003;63:1727–30.
- Lewis JD, Ng K, Hung KE, et al. Detection of proximal adenomatous polyps with screening sigmoidoscopy—a systematic review and meta-analysis of screening colonoscopy. *Arch Intern Med* 2003;163:413–20.
- Roy HK, Kim YL, Liu Y, et al. Risk stratification of colon carcinogenesis through enhanced backscattering spectroscopy analysis of the uninvolved colonic mucosa. *Clin Cancer Res* 2006;19:961–8.
- Roy HK, Liu Y, Wali RK, et al. Four-dimensional elastic light-scattering fingerprints as preneoplastic markers in the rat model of colon carcinogenesis. *Gastroenterology* 2004;126:1071–81.
- Matsubayashi H, Sato N, Brune K, et al. Age- and disease-related methylation of multiple genes in non-neoplastic duodenum and in duodenal juice. *Clin Cancer Res* 2005;11:573–83.
- Roy HK, Iversen P, Hart J, et al. Down-regulation of SNAIL suppresses MIN mouse tumorigenesis: modulation of apoptosis proliferation, and fractal dimension. *Mol Cancer Ther* 2004;3:1159–65.
- Roy HK, Kim YL, Wali RK, et al. Spectral markers in preneoplastic intestinal mucosa: an accurate predictor of tumor risk in the MIN mouse. *Cancer Epidemiol Biomarkers Prev* 2005;14:1639–45.
- Kim YL, Liu Y, Wali RK, et al. Simultaneous measurement of angular and spectral properties of light scattering for characterization of tissue microarchitecture and its alteration in early precancer. *IEEE J Sel Top Quantum Electron* 2003;9:243–56.
- Liu Y, Kim YL, Li X, Backman V. Investigation of depth selectivity of polarization gating for tissue characterization. *Opt Express* 2005;13:601–11.
- Liu Y, Kim YL, Backman V. Development of a bioengineered tissue model and its application in the investigation of the depth selectivity of polarization gating. *Appl Opt* 2005;44:2288–99.
- Backman V, Gurjar R, Badizadegan K, et al. Polarized light scattering spectroscopy for quantitative measurement of epithelial cellular structures *in situ*. *IEEE J Sel Top Quantum Electron* 1999;5:1019–26.
- Kim YL, Liu Y, Turzhitsky VM, et al. Coherent backscattering spectroscopy. *Opt Lett* 2004;29:1906–8.
- Kim YL, Liu Y, Turzhitsky VM, et al. Depth-resolved low-coherence enhanced backscattering. *Opt Lett* 2005;30:741–3.
- Wax A, Yang CH, Backman V, et al. Cellular organization and substructure measured using angle-resolved low-coherence interferometry. *Biophys J* 2002;82:2256–64.
- Rammal R, Doucot B. Invariant imbedding approach to localization. I. General framework and basic equations. *J Phys* 1987;48:509–26.
- Feng SC, Kane C, Lee PA, Stone AD. Correlations and fluctuations of coherent wave transmission through disordered media. *Phys Rev Lett* 1988;61:834–7.
- Wax A, Yang CH, Muller MG, et al. *In situ* detection of neoplastic transformation and chemopreventive effects in rat esophagus epithelium using angle-resolved low-coherence interferometry. *Cancer Res* 2003;63:3556–9.
- Liu Y. Elastic light scattering fingerprinting for tissue characterization [dissertation]. Evanston (IL): Northwestern University; 2006.
- Maitra A, Ashfaq R, Gunn CR, et al. Cyclooxygenase 2 expression in pancreatic adenocarcinoma and pancreatic intraepithelial neoplasia—an immunohistochemical analysis with automated cellular imaging. *Am J Clin Pathol* 2002;118:194–201.
- Watanabe H, Yamaguchi Y, Ha A, et al. Quantitative determination of K-ras mutations in pancreatic juice for diagnosis of pancreatic cancer using hybridization protection assay. *Pancreas* 1998;17:341–7.
- Shamsuddin AM, Tyner GT, Yang GY. Common expression of the tumor-marker D-galactose-β-1-3-N-acetyl-D-galactosamine by different adenocarcinomas—evidence of field-effect phenomenon. *Cancer Res* 1995;55:149–52.